Cross section and analyzing powers for ^{6}Li-^{4}He elastic scattering at 5.5 and 19.6 MeV

E. A. George,[1,2] D. D. Pun Casavant,[1] and L. D. Knutson[1]
[1]*Physics Department, University of Wisconsin, Madison, Wisconsin 53706*
[2]*Department of Physics, University of Wisconsin-Whitewater, Whitewater, Wisconsin 53190*
(Received 21 January 1997)

Measurements of the differential cross section and the analyzing powers iT_{11}, T_{20}, T_{21}, and T_{22} for ^{6}Li-^{4}He elastic scattering have been made at incident ^{6}Li energies of 5.5 and 19.6 MeV. The measurements cover an angular range of $\theta_{\text{c.m.}}=18.8°-165°$ at 19.6 MeV, and $\theta_{\text{c.m.}}=37.8°-160°$ at 5.5 MeV. The data are compared to several different optical model calculations. Also, the calibration of a $^6\vec{\text{Li}}$ polarimeter, which employs $^6\vec{\text{Li}}$-^{4}He elastic scattering, is described. [S0556-2813(97)05907-4]

PACS number(s): 24.70.+s, 25.70.Bc

I. INTRODUCTION

The elastic scattering of $^6\vec{\text{Li}}$ by ^{4}He is of interest for a variety of reasons. The process has previously been studied for clues to the origin of its large vector analyzing powers [1], and the fact that the analyzing powers are large makes the reaction useful as a beam polarization monitor [2]. Recently, Green *et al.* [3] reported measurement of a complete set of vector and tensor analyzing powers and cross sections for this reaction, at an incident ^{6}Li energy of 27.8 MeV ($E_{\text{c.m.}}=11.1$ MeV). They have used these measurements to investigate the spin dependence of ^{6}Li-^{4}He elastic scattering and the spin structure of the ^{6}Li nucleus.

Our motivation for undertaking the present experiment was to obtain data for the purpose of determining the asymptotic D-state to S-state ratio of the $^6\text{Li}\rightarrow\alpha+d$ cluster wave function. We had intended to determine this quantity by the pole extrapolation method [4], but unfortunately this approach has not led to unambiguous results. We are currently developing an alternative method of determining the D- to S-state ratio from the data, and will describe that work elsewhere.

The purpose of this paper is to report measurements of the differential cross section and vector and tensor analyzing powers for ^{6}Li-^{4}He elastic scattering at incident ^{6}Li energies of 5.5 and 19.6 MeV ($E_{\text{c.m.}}=2.2$ and 7.8 MeV). The measurements are compared with predictions obtained from the optical model potentials of Ref. [3]. In addition to reporting these measurements, we also describe the calibration of a $^6\vec{\text{Li}}$ polarimeter which employs $^6\vec{\text{Li}}$-^{4}He scattering at an incident $^6\vec{\text{Li}}$ energy of about 13 MeV.

II. DESCRIPTION OF THE EXPERIMENT

A. Cross-section measurements

1. 19.6 MeV

The measurements were carried out at the University of Wisconsin tandem accelerator laboratory. An unpolarized beam of ^{6}Li ions from a negative-ion sputter source [5] was accelerated, momentum analyzed by a 90° bending magnet, and transported to a 1-m diameter scattering chamber. The experimental arrangement was similar to that described in Ref. [6].

Beam collimation was provided by a 1 mm wide by 2 mm high beam defining aperture located 35.6 cm from the center of the scattering chamber, followed by a pair of antiscattering slits. A 0.5 μm Ni entrance foil located 35.8 cm from the center of the chamber was used to separate the chamber from the beamline vacuum.

The chamber was filled with 150 Torr natural helium gas of 99.999% purity. The gas was continuously added to the chamber through a long metal capillary tube and pumped out through a needle valve, with the flow rate set so that the gas was replaced every 4–6 h. The chamber pressure was monitored continuously and the rate at which gas was added was electronically controlled by adjusting the temperature of the capillary. In this way, the chamber pressure was maintained to ± 0.05 Torr. The chamber temperature was measured using a thermometer placed in good thermal contact with the top of the scattering chamber. Corrections to the gas density for variations in temperature were less than 0.5%.

Silicon surface-barrier detectors were used to detect the reaction products. The detectors were placed symmetrically to the left and right of the incident beam, with three detectors on each side, spaced 10° apart. Measurements were made at lab angles ranging from 7.5° to 62.5°. Detector thicknesses were chosen so that ^{6}Li and α particles were stopped in the detector, whereas protons and deuterons were not. Each detector was located about 26 cm from the center of the chamber, and was equipped with front and back slits to define the angular range viewed, as well as with antiscattering slits. The angular acceptance ranged from $\pm 0.34°$ to $\pm 0.68°$.

In order to determine the geometric factors for the detector slit sets, we used a traveling microscope to measure the dimensions for one slit set. Then we obtained elastic-scattering data at a lab angle of 35° for all detector and slit combinations used. The yields for each slit set at this angle, normalized to the integrated charge, were compared to the normalized yield for the measured slit set in order to determine the rest of the geometric factors.

Signals from the detectors were amplified and shaped and passed through analog-to-digital converters interfaced to an online computer. A pulser signal triggered at a rate proportional to the instantaneous beam current was passed through the detector electronics, and dead time in the electronics was determined by measuring the fraction of these pulser counts lost.

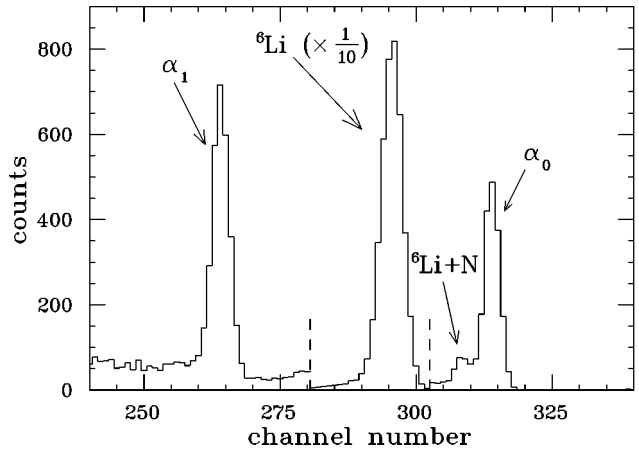

FIG. 1. Typical pulse-height spectrum for ^{6}Li-^{4}He elastic scattering at 19.6 MeV at $\theta_{lab}=10°$. A 1.6 mg/cm^2 polyethylene slowing foil was placed in front of the detector to separate the elastically scattered ^{6}Li particles from the recoil α particles.

A typical forward-angle spectrum at an incident ^{6}Li energy of 19.6 MeV is shown in Fig. 1. At forward angles, a small contaminant peak from ^{6}Li-N elastic scattering is present, but is reasonably well separated from the peaks of interest. Peak-to-background ratios at this energy were 300:1 or better at all angles. At lab angles between 7.5° and 15°, a 1.6 mg/cm^2 polyethylene foil was placed in front of the detectors to separate the ^{6}Li elastic-scattering peak from the recoil α peak.

The absolute beam current was measured using a Faraday cup under vacuum, placed directly behind the scattering chamber. A 2.54 μm Havar foil separated the Faraday cup vacuum from the chamber. Due to multiple scattering in this foil, the Faraday cup did not collect all of the beam on target. In order to determine the fraction of charge collected, we installed a movable Faraday cup in the scattering chamber, and evacuated the chamber. First, charge was collected by this internal cup for 30 s. Then, the internal cup was swung out of the way, and charge was collected by the Faraday cup behind the chamber for another 30 s. This process was repeated four times, and the fraction of total charge collected by the cup behind the chamber was determined to be 0.645 ± 0.016. A small amount of additional lost charge results from multiple scattering in the target gas. The systematic error in the measured cross section due to this effect was calculated to be 1.2%.

We obtained the cross section directly from the measured yields, integrated charge, and detector geometry, and from the target number density, which was calculated from the measured gas pressure and temperature. Dead-time corrections were typically less than 1%. A peak-fitting program was used to obtain the peak sums in cases where background was not negligible.

2. 5.5 MeV

At this energy, a setup similar to that at 19.6 MeV was used. The major differences were that the helium gas pressure was 50 Torr instead of 150 Torr, and the scattering chamber was separated from the Faraday cup by a 0.5 μm Ni foil instead of by the thicker Havar foil. Measurements were made at lab angles from 10° to 45°.

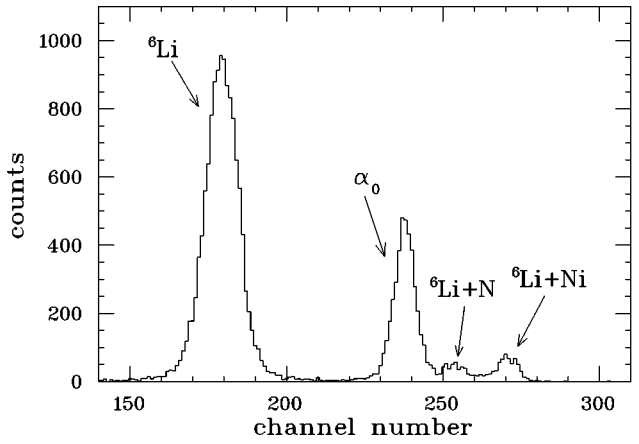

FIG. 2. Sample spectrum for ^{6}Li-^{4}He elastic scattering at 5.5 MeV at $\theta_{lab}=25°$ with no slowing foil in front of the detector.

Figure 2 shows a representative forward-angle spectrum at this energy. Besides the contaminant peak from ^{6}Li-N elastic scattering, there is an additional contaminant peak at forward angles due to ^{6}Li scattering from the Ni entrance foil, followed by small-angle scattering in the target gas. In order to resolve the α peak at angles forward of 22.5°, a 1.6 mg/cm^2 polyethylene foil was placed over the detector slits to stop all ^{6}Li particles. Peak sums for the elastic ^{6}Li group for lab angles between 17.5° and 22.5° were obtained by taking additional runs with no foil in front of the detectors. A few runs were also taken between 15° and 25° with a 100 μg/cm^2 carbon foil, in order to separate the ^{6}Li peak of interest from the recoil α peak. Forward of 15°, the ^{6}Li peak was too close to the contaminant peaks to be useable. Peak-to-background ratios at 5.5 MeV were 30:1 or better at all angles.

At this energy, we determined the cross section normalization in the following way. We took data at a lab angle of 35° with 0.5 Torr natural xenon gas and 45 Torr helium gas in the scattering chamber. These gas pressures were chosen to ensure that the energy of the ^{6}Li beam at the center of the chamber was the same as when 50 Torr of helium gas was in the chamber. Then, with only helium gas in the chamber, we obtained measurements at 35° for all detector and slit combinations. We then normalized the ^{6}Li-^{4}He cross sections to the calculated ^{6}Li-Xe cross section, which was assumed to be purely Rutherford. Dead-time corrections were less than 1%, and background corrections were less than 3%.

B. Analyzing power measurements

A $^6\vec{\text{Li}}$ beam from a colliding-beam polarized ion source [7] was used to obtain analyzing powers. The procedures used to determine analyzing powers are similar to those described in detail in Ref. [6]. Briefly, for a reaction induced by a beam of polarized spin-1 particles, the yield for a detector on the left or right side of the beam can be written

$$Y_{l,r}=Y^o_{l,r}(1+t_{20}T_{20}\pm 2t_{21}T_{21}+2t_{22}T_{22}\pm 2it_{11}iT_{11}), \tag{1}$$

where the upper and lower signs correspond to the left and right detector, respectively. Here, $Y^o_{l,r}$ is the yield obtained from an unpolarized beam, the T_{kq} are the analyzing powers

for the reaction, and the t_{kq} are the corresponding beam polarization moments. (Throughout this paper, t_{21}, t_{22}, and it_{11} should be understood to refer to the real parts of these beam moments.) To obtain the analyzing powers, one needs to measure only relative yields and the beam polarization moments.

For each angle set, data were taken for three different polarization states. For each state, the polarization parameters were chosen so that one or two beam moments were large, while the others were close to zero. The typical ''large'' beam moments for the three states were: $t_{20} \approx \pm 0.49$; t_{21} and $t_{22} \approx \pm 0.24$; and $it_{11} \approx \pm 0.43$. During each run, the sign of the beam polarization was changed at intervals of less than 1 s by switching the radio-frequency transitions at the ion source. Analyzing powers were obtained from the measured yields and beam moments using an iterative procedure described in Ref. [6].

1. 19.6 MeV

At 19.6 MeV, the experimental setup was similar to that used to measure the cross section, except for the addition of a $^6\vec{\mathrm{Li}}$ polarimeter immediately behind the scattering chamber. Details of the construction and calibration of the polarimeter are given in the following section. A 2.54 μm thick Havar foil was used to separate the main scattering chamber from the polarimeter, which was filled with 1 atm of natural helium gas. A 4 μm Havar foil was placed in front of the exit foil to degrade the energy of the beam entering the polarimeter to a nominal 14.6 MeV, the energy at which the polarimeter was calibrated. A Faraday cup located at the back of the polarimeter was used to monitor beam current. Because the gas in the polarimeter was partially ionized by the beam, an absolute determination of beam current could not be obtained. However, because our method of data analysis requires only the relative integrated charge for the positive and negative spin states, and because fast switching between spin states was employed, this arrangement was adequate.

A background correction was applied to the data where necessary. In almost all cases, this correction to the analyzing powers was less than ± 0.005, although in one case it was as large as 0.104. The dead-time correction was less than ± 0.002.

2. 5.5 MeV

At a beam energy of 5.5 MeV, some modifications to the setup were necessary because the lower-energy $^6\vec{\mathrm{Li}}$ beam rapidly depolarizes in the target gas, due to multiple pickup and stripping of electrons. In order to reduce the amount of

$T_{20}=-0.534\pm0.006$ and $T_{22}=0.115\pm0.004$, where the errors include normalization uncertainties as well as statistical uncertainties.

These measurements, along with Eqs. (2) and (3), allowed us to determine the $^6\vec{\text{Li}}$ polarimeter analyzing powers T_{20} and T_{22} in the following way. We placed a 2.54 cm diameter gas cell filled with 1 atm of 98% pure deuterium gas in the main scattering chamber. Detectors were placed left, right, above, and below the beam, at $\theta_{\text{lab}}=55°$ ($\theta_{\text{c.m.}}=90°$). This arrangement permits determination of the $^6\vec{\text{Li}}$ beam moments t_{20} and t_{22} for any given run. The energy of the $^6\vec{\text{Li}}$ beam was chosen to give $E_{\text{Li}}=17.5$ MeV at the reaction center, corresponding to $E_{\text{c.m.}}=4.39$ MeV. After passing through the gas cell, the beam entered the polarimeter with an energy degraded to the calibration energy, 14.6 MeV. Measurements were obtained with t_{20}, A_{xx}, and A_{yy} polarized beams, allowing us to make multiple determinations of polarimeter T_{20} and T_{22} analyzing powers. Because these determinations with different beam polarizations are statistically independent, we took weighted averages of the individual determinations as our result.

Because there are no general relations such as Eqs. (2) and (3) for T_{21} and iT_{11}, these polarimeter analyzing powers cannot be determined in the same way. Instead, we used known properties of the polarized ion source and beam transport system, along with the T_{20} and T_{22} measurements, to determine T_{21} and iT_{11}. Assuming that the beam polarization has an axis of symmetry, the beam moments are given by [11]

$$t_{20}=\frac{1}{2}\tau_{20}(3\cos^2\beta-1), \tag{4a}$$

$$t_{21}=\sqrt{\frac{3}{2}}\tau_{20}\sin\beta\cos\beta\sin\phi, \tag{4b}$$

$$t_{22}=-\sqrt{\frac{3}{8}}\tau_{20}\sin^2\beta\cos2\phi, \tag{4c}$$

$$it_{11}=\frac{1}{\sqrt{2}}\tau_{10}\sin\beta\cos\phi, \tag{4d}$$

where β is the angle between the spin symmetry axis and the incident beam direction, and ϕ is the azimuthal angle of the spin symmetry axis measured from the vertical (see Ref. [11]).

The T_{21} analyzing powers were determined by taking polarimeter data for a series of runs having essentially pure tensor polarization, with $\phi=90°$ to maximize t_{21} and t_{22}. The angle β was varied between 15° and 120° by changing the electric and magnetic-field settings of a Wien filter located between the ion source and the accelerator. We then fit the measured values of t_{20} and t_{22}, treating τ_{20}, the Wien filter calibration (that is, the dependence of β on the field settings), and the deviation of the alignment axis from the initial beam direction as free parameters. Then by using Eq. (4b), we obtained t_{21} for each run, which in turn allowed us to determine the polarimeter T_{21} analyzing powers.

To obtain the vector analyzing power, we made use of the fact that the efficiencies of the polarized source radio-frequency transition units can be calculated once τ_{20} is known. From t_{20} runs, we determined that τ_{20} was about 81% of its theoretical maximum for one spin state and about 95% for the other. Based on these numbers, and assuming that the depolarization is dominated by inefficiencies in the transition units, we calculated that the vector polarization in the strong-field state should be about 88% of the theoretical maximum. This corresponds to a τ_{10} of approximately 0.72. Because it is not clear what the actual depolarization mechanisms are, we take the error in τ_{10} to be fairly large, $\pm10\%$. By assuming that $\beta=90°$ and $\phi=180°$ for it_{11} runs, we were then able to calculate it_{11} for these runs. The polarimeter iT_{11} analyzing powers were then calculated by assuming that other beam moments were zero for the iT_{11} runs. The results were checked using data from an A_{yy} run. Both methods produced statistically equivalent results, and a weighted average of the two was taken for the final iT_{11} analyzing powers.

Finally, using these analyzing powers, we recalculated beam moments for all types of runs and verified that all beam moments assumed to be small were statistically equivalent to zero. The polarimeter calibration uncertainties are estimated to be roughly 3% for T_{20}, 7% for T_{21}, 5% for T_{22}, and 11% for iT_{11}.

During the measurements of the ^{6}Li-^{4}He analyzing powers, a small error was made in matching the beam energy in the polarimeter to the calibration energy. This error was discovered only after the experiment was completed, and so it was necessary to correct the measured analyzing powers. This correction was made by measuring the polarimeter analyzing powers at several energies near the energy at which the polarimeter had been calibrated and then interpolating to find the analyzing powers at the actual beam energy. Some of the data were reanalyzed using the correct analyzing powers and correction factors were derived for the rest of the data. The resulting corrections were less than ±0.040 at 19.6 MeV, where the error in energy matching was 340 keV, and less than ±0.010 at 5.5 MeV, where the error in energy matching was 100 keV.

III. RESULTS

Cross-section and analyzing power measurements at incident ^{6}Li energies of 19.6 and 5.5 MeV are shown in Figs. 3 and 4, respectively. We note that the data will be deposited in the National Nuclear Data Center's online nuclear reaction database.

For the cross-section measurements at 19.6 MeV, error bars include statistical errors in the peak sums, in measurements of detector geometry, in integrated charge, and in the fit at angles where peak fitting was necessary. The normalization error in the measured cross section is 6%. This error is due to uncertainty in peak sum limits, in absolute integrated charge, and in the detector geometry measurements. The error bars shown for the analyzing powers at this energy include statistical uncertainties in peak sums, in the beam moments, and in the background subtraction. In addition to the statistical errors, there is an overall normalization error arising from uncertainties in the polarimeter analyzing pow-

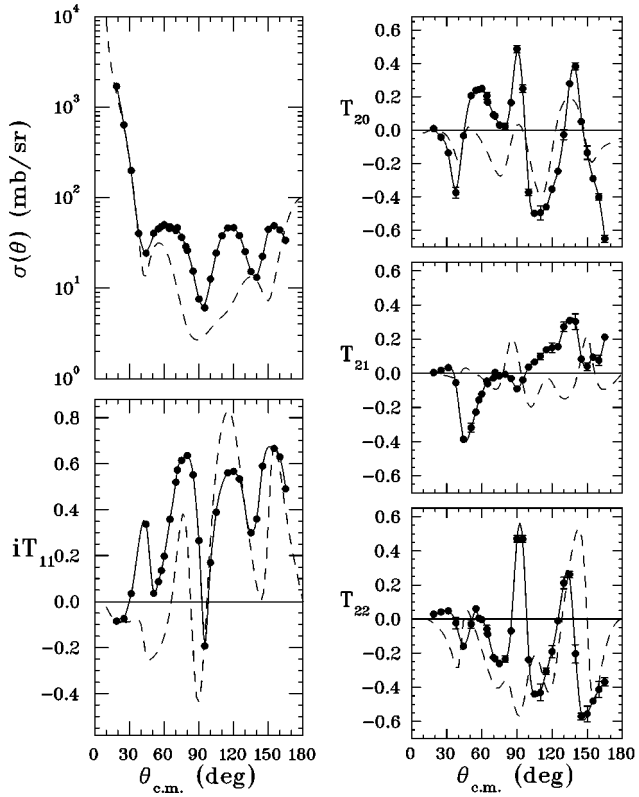

FIG. 3. Differential cross section and the four analyzing powers for ^{6}Li-^{4}He elastic scattering at $E_{\rm Li}=19.6$ MeV. The solid lines are a guide for the eye. The dashed lines are optical model calculations using parameter set 1 of Ref. [3].

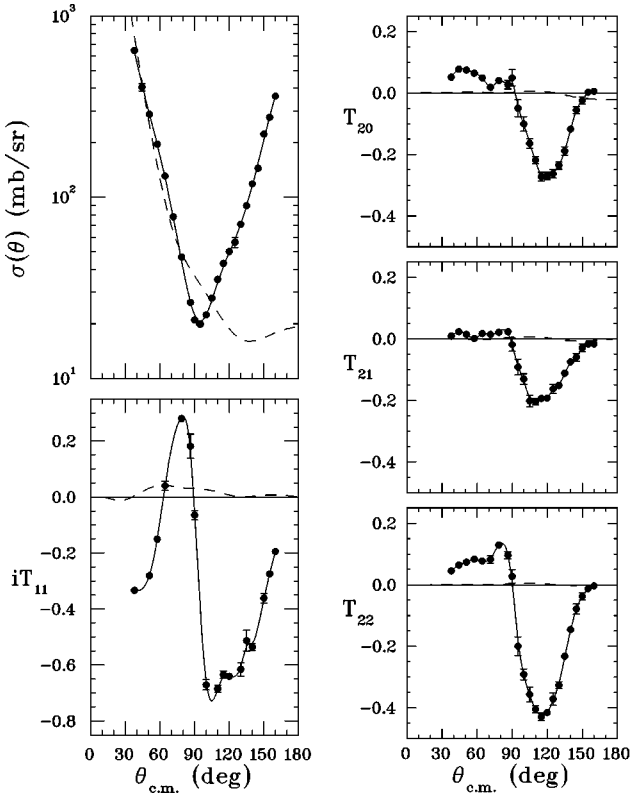

FIG. 4. Differential cross section and the four analyzing powers for ^{6}Li-^{4}He elastic scattering at $E_{\rm Li}=5.5$ MeV. The solid lines are a guide for the eye. The dashed lines are optical model calculations using parameter set 1 of Ref. [3].

ers and in the correction for the error in matching the beam energy to the polarimeter calibration energy. The normalization error is estimated to be 8% for T_{20}, 12% for T_{21}, 9% for T_{22}, and 12% for iT_{11}.

For the 5.5 MeV cross-section measurements shown in Fig. 4, there is a 4% normalization error, arising from finite peak sum limits and from uncertainty in the normalization to the ^{6}Li-Xe cross section. For analyzing powers at this energy, the normalization error is due to uncertainty in the polarimeter analyzing powers, and to uncertainty in the depolarization factors. Uncertainty in the correction for matching the beam energy to the polarimeter calibration energy is negligible. The normalization error is estimated to be 12% for T_{20}, 10% for T_{21}, 9% for T_{22}, and 12% for iT_{11}.

IV. DISCUSSION

A comparison of the 19.6 MeV vector analyzing powers to the 18.3 and 21.3 MeV iT_{11} data of Ref. [1] shows that the new vector analyzing power measurements are quite similar in shape and magnitude to the older ones. This is as expected, because the energy dependence of iT_{11} is weak in this energy range [1]. The 19.6 MeV analyzing powers are qualitatively similar to those measured at 27.8 MeV by Green *et al.* [3], in that all analyzing powers are large (except for T_{21} at 27.8 MeV), and have a good deal of angular structure. The analysis of Ref. [3] indicates that the spin-orbit potential, exchange interactions, and channel coupling all contribute to the analyzing powers at 27.8 MeV.

Because of the relatively weak energy dependence of the cross section and vector analyzing powers in the 18–30 MeV lab energy range, it is instructive to compare our measurements to optical model calculations using parameters that fit the 27.8 MeV data [3]. In Fig. 3, the 19.6 MeV data are shown along with an optical model calculation using the set 1 parameters of Ref. [3]. This set includes real and imaginary central potentials, a spin-orbit and a tensor potential, and a J-dependent form factor in the imaginary central potential (to simulate channel-coupling effects). Green *et al.* found that this set of parameters gave a good fit to forward-angle ($<90°$) cross-section and analyzing power data at 27.8 MeV. Our 19.6 MeV data are not as well-described by the optical model calculations as the 27.8 MeV data are, although the general shapes of all but the T_{21} analyzing powers are in rough agreement with the data. Figure 5 shows the results of calculations using parameter sets 2 and 3 from Ref. [3]. Set 2 has no tensor potential or J dependence, and gave a good fit to the 27.8 MeV cross-section data. Set 3 has the same types of parameters as set 1, but was found to give a somewhat better fit to the back angle data at 27.8 MeV than did set 2 or set 1. Again, at 19.6 MeV, neither set 2 nor set 3 gives a satisfactory fit to the whole range of data, although set 3 gives a better fit to T_{21} than do the other sets. We have found that it is possible to improve the cross-section fits somewhat by using slightly different parameters, but, as with the 27.8 MeV data, the back-angle cross-section data generally cannot be fit well.

At 5.5 MeV, the cross section and analyzing powers have a much simpler structure than at 19.6 MeV. The cross section also shows a strong back-angle peaking, which is under-

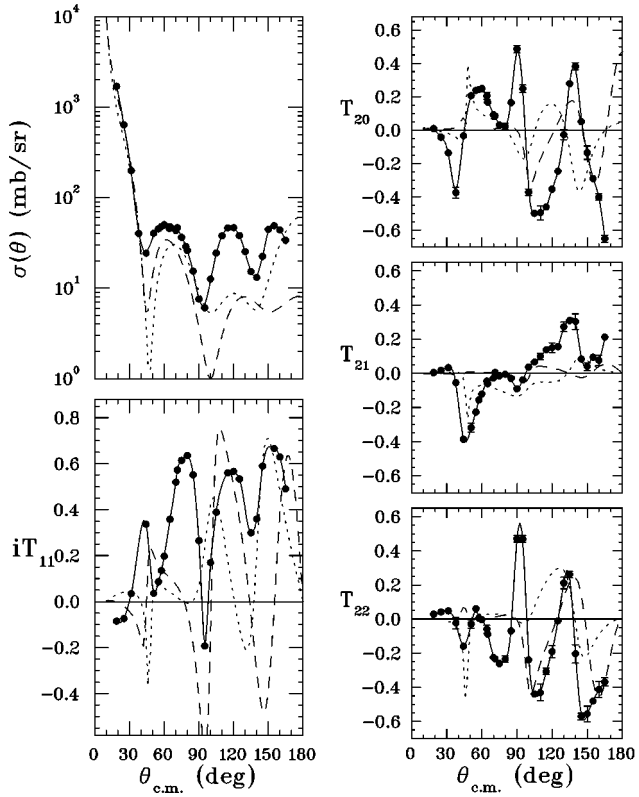

FIG. 5. Differential cross section and the four analyzing powers for ^{6}Li-^{4}He elastic scattering at $E_{\rm Li}=19.6$ MeV, with optical model calculations using parameter set 2 (dashed lines) and parameter set 3 (dotted lines) of Ref. [3].

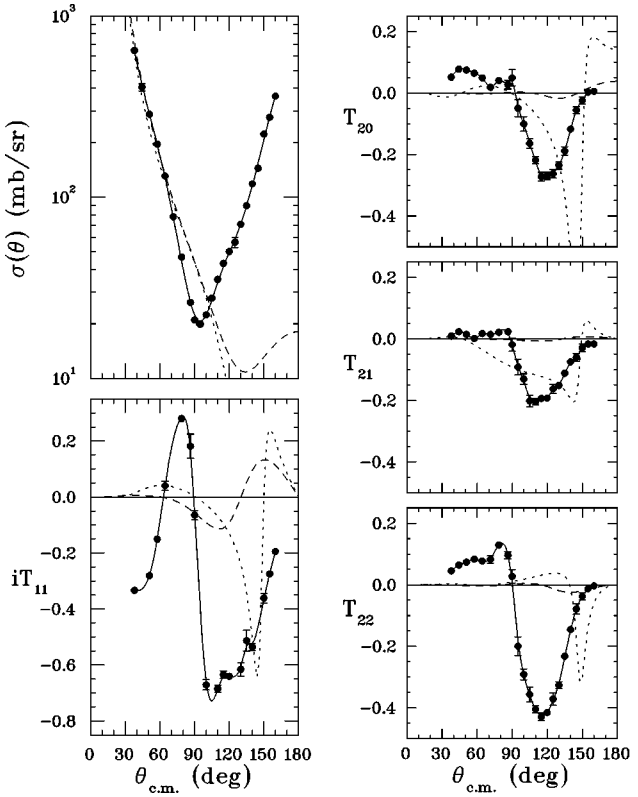

FIG. 6. Differential cross section and the four analyzing powers for ^{6}Li-^{4}He elastic scattering at $E_{\rm Li}=5.5$ MeV, with optical model calculations using parameter set 2 (dashed lines) and parameter set 3 (dotted lines) of Ref. [3].

stood as being due to the process of deuteron exchange between the two α-particle clusters [12]. It can be seen in Figs. 4 and 6 that the back-angle cross section is not fit well by the optical model potential parameters of Ref. [3]. Although it is possible to produce better optical-model fits to the 5.5 MeV data (particularly the forward-angle cross section), the back-angle data are still not well fit. If deuteron exchange does play an important role at the back angles, it is reasonable to suppose that the back-angle analyzing powers are sensitive to details of the internal structure of ^{6}Li. In that case, these lower-energy measurements may be particularly useful for investigating the spin degrees of freedom of ^{6}Li.

ACKNOWLEDGMENTS

We thank the students and staff of the University of Wisconsin-Madison nuclear physics group for their assistance in taking data. We also thank Sean Nimm for his help in performing the optical model calculations. This work was supported in part by the National Science Foundation and by a University of Wisconsin-Whitewater Research Grant.

[1] P. Egelhof, J. Barrette, P. Braun-Munzinger, W. Dreves, C. K. Gelbke, D. Kassen, E. Steffens, W. Weiss, and D. Fick, Phys. Lett. **84B**, 176 (1979).

[2] A. J. Mendez, E. G. Myers, K. W. Kemper, P. L. Kerr, E. L. Reber, and B. G. Schmidt, Nucl. Instrum. Methods Phys. Res. A **329**, 37 (1993).

[3] P. V. Green, K. W. Kemper, P. L. Kerr, K. Mohajeri, E. G. Myers, D. Robson, K. Rusek, and I. J. Thompson, Phys. Rev. C **53**, 2862 (1996).

[4] R. D. Amado, M. P. Locher, and M. Simonius, Phys. Rev. C **17**, 403 (1978).

[5] G. T. Caskey, Ross A. Douglas, H. T. Richards, and H. Vernon Smith, Jr., Nucl. Instrum. Methods **157**, 1 (1978).

[6] J. Sowinski, D. D. Pun Casavant, and L. D. Knutson, Nucl. Phys. **A464**, 233 (1987).

[7] G. S. Masson, T. Wise, P. A. Quin, and W. Haeberli, Nucl. Instrum. Methods Phys. Res. A **242**, 196 (1986).

[8] R. R. Cadmus, Jr. and W. Haeberli, Nucl. Instrum. Methods **192**, 403 (1975).

[9] D. Fick, Z. Phys. **237**, 131 (1970).

[10] K. Stephenson and W. Haeberli, Nucl. Instrum. Methods **169**, 483 (1980).

[11] W. Haeberli, in *Nuclear Spectroscopy and Reactions*, edited by J. Cerny (Academic, New York, 1974), Pt. A, p. 151.

[12] P. Truoel and W. Bierter, Phys. Lett. **29B**, 21 (1969).